Topological Correspondence between Hermitian and Non-Hermitian Systems: Anomalous Dynamics

Jong Yeon Lee, Junyeong Ahn, Hengyun Zhou, and Ashvin Vishwanath

Phys. Rev. Lett. **123**, 206404 — Published 13 November 2019

DOI: 10.1103/PhysRevLett.123.206404

Topological Correspondence between Hermitian and Non-Hermitian Systems: Anomalous Dynamics

Jong Yeon Lee,[1] Junyeong Ahn,[2,3,4] Hengyun Zhou,[1] and Ashvin Vishwanath[1]

[1] *Department of Physics, Harvard University, Cambridge, Massachusetts 02138, USA*
[2] *Department of Physics and Astronomy, Seoul National University, Seoul 08826, Korea*
[3] *Center for Correlated Electron Systems, Institute for Basic Science (IBS), Seoul 08826, Korea*
[4] *Center for Theoretical Physics (CTP), Seoul National University, Seoul 08826, Korea*

(Dated: October 24, 2019)

The hallmark of symmetry-protected topological (SPT) phases is the existence of anomalous boundary states, which can only be realized with the corresponding bulk system. In this work, we show that for every Hermitian anomalous boundary mode of the ten Altland-Zirnbauer classes, a non-Hermitian counterpart can be constructed, whose long time dynamics provides a realization of the anomalous boundary state. We prove that the non-Hermitian counterpart is characterized by a point-gap topological invariant, and furthermore, that the invariant exactly matches that of the corresponding Hermitian anomalous boundary mode. We thus establish a correspondence between the topological classifications of $(d+1)$-dimensional gapped Hermitian systems and d-dimensional point-gapped non-Hermitian systems. We illustrate this general result with a number of examples in different dimensions. This work provides a new perspective on point-gap topological invariants in non-Hermitian systems.

Introduction— In the last few decades, topology has emerged as a central theme in the study of condensed matter physics. The interplay of symmetry and topology has led to a wide variety of interesting phenomena, most notably that of symmetry-protected topological phases (SPTs) [1–4]. One of the key physical signatures of SPTs are their anomalous boundary states, which can only be realized as d-dimensional boundary states of a $(d+1)$-dimensional topological bulk, and cannot appear in a d-dimensional bulk model.

Recently, the study of topological phenomena has also been extended to non-Hermitian systems [5–52], which are naturally realized in classical optical systems with gain and loss [34, 53–58], superconducting vortices [6], ring neural networks [59], bosonic superconducting systems [15, 60], or magnon band structures [61, 62], and has also been proposed to be relevant to electronic systems with finite quasiparticle lifetime [13, 23, 63, 64]. In particular, with a suitable generalization of the gap condition [14], SPTs can be generalized to the non-Hermitian setting and the well-known ten-fold way classification for non-interacting fermionic topological phases under the Altland-Zirnbauer (AZ) symmetry classes [1, 65, 66] can be extended to the 38 non-Hermitian Bernard-LeClair (BL) symmetry classes [15, 67–70]. Interestingly, the classification of non-Hermitian SPTs also exhibits a periodic structure similar to Hermitian systems [14, 69, 70], both in symmetry class and spatial dimension, and certain characteristics of the 1D non-Hermitian models studied are reminiscent of boundary states of 2D Hermitian models with related symmetries [69, 71]. As an example, the boundary of a 2D quantum Hall system hosts anomalous chiral edge states, which bears some resemblance to the 1D non-Hermitian chiral hopping model, as shown in Fig. 1(c). This raises the question of whether

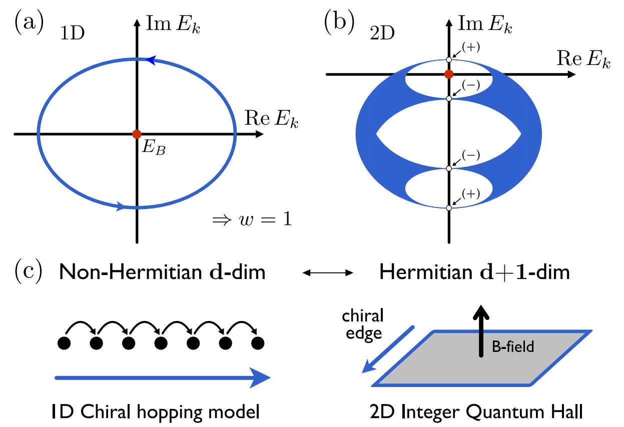

FIG. 1. (a) Dispersion for the 1D chiral hopping model in the complex plane. The topological invariant w is defined with respect to E_B as in Eq. (3). Depending on the value of E_B and other parameters, w can differ. In this case, $w = 1$. (b) Dispersion for the 2D model in Eq. (19) that resembles the surface of a 3D chiral topological insulator. Here, $\gamma_{\boldsymbol{k}} = 2\cos k_x + \cos k_y$, $b_{1,\boldsymbol{k}} = \sin k_x$, $b_{2,\boldsymbol{k}} = \sin k_y$, $b_{3,\boldsymbol{k}} = 0$. Each white dot represents a Dirac cone with $\pm$ chirality. In this case, depending on E_B, the topological invariant can be $1, 0, -1$. (c) The 1D system characterized by $w \in \mathbb{Z}$ in the chiral hopping model corresponds to the edge of a 2D system characterized by an integer quantum Hall state with Chern number $n = w \in \mathbb{Z}$.

there exists a more general correspondence between the anomalous boundary states of a Hermitian system, and the dynamics of a corresponding non-Hermitian system with one dimension lower.

In this Letter, we establish a correspondence between the ten-fold-way topological classification of non-interacting Hermitian systems in $(d+1)$ dimensions and the point-gap topology of certain non-Hermitian systems in d dimensions, and describe how this gives a possible interpretation to the long-time dynamics of non-Hermitian models as a *dynamical anomaly*, in direct relation to the anomalous boundary physics of Hermitian systems. We motivate this by introducing a 1D chiral hopping non-Hermitian model and examining the relation between non-Hermitian band topology and anomalous chiral modes in the long-time limit. We then generalize this to other symmetry classes, and prove the above correspondence in both the topological classification as well as the explicit realization of anomalous dynamics.

Emergence of chiral fermions in a 1D non-Hermitian system— We start by considering an example to motivate and illustrate the main idea of the correspondence. Consider the following single-band non-Hermitian Hamiltonian in one dimension [6, 14]:

$$H = \sum_r \left(t_L c_r^\dagger c_{r+1} + t_R c_{r+1}^\dagger c_r \right), \tag{1}$$

where $t_R \neq t_L$. Under the Fourier transformation $c_r = \sum_k c_k e^{ikr}$, the k-space Hamiltonian is given by $H_k = (t_L + t_R)\cos k + i(t_L - t_R)\sin k$. Thus, the energy dispersion E_k forms an ellipse in the complex energy plane [Fig. 1(a)]. For a positive (negative) $t_L - t_R$, the band winds around the origin in the counterclockwise (clockwise) direction. The group velocity v_k of a wave packet centered at k is given by [14]

$$v_k = \mathrm{Re}\,\frac{1}{\hbar}\frac{\partial E_k}{\partial k} = -(t_L + t_R)\sin k, \tag{2}$$

since the imaginary part of $\partial_k E_k$ does not affect the propagation velocity of the wave packet.

On top of this, there is an additional ingredient that influences the dynamics of a non-Hermitian system, the imaginary part of the energy which causes certain eigenstates to grow or decay with $\mathrm{Im}\,E_k = (t_L - t_R)\sin k$. If we inspect the dynamics at real energy near zero, then there may exist two modes: left and right propagating modes with $k = \pm\pi/2$. While the left-propagating mode has a positive $\mathrm{Im}\,E_k$, the right-propagating mode has a negative $\mathrm{Im}\,E_k$. Therefore, if we excite the system with a frequency $\omega \sim 0$, generically both counter-propagating modes will be excited, but the right-propagating mode will die out after a timescale $\tau_0 \gg \hbar/\,\mathrm{Im}\,E_k$. At long times, we will thus observe chiral dynamics in the system with only a left-propagating mode, a scenario which cannot be realized in any 1D Hermitian system.

Non-Hermitian Topology with Complex Point Gap— The above chiral dynamics can be directly connected to the topological properties of the non-Hermitian band structure. Here, band topology is defined by the complex point energy gap constraint: for a given complex base energy E_B, two band structures are topologically equivalent if and only if one can be deformed to the other without crossing E_B during the deformation [14, 69, 70]. In this context, $\mathrm{Re}\,E_B$ and $\mathrm{Im}\,E_B$ are the real energy window and overall loss/gain level we are referenced to, respectively. Note that the choice of point-gap non-Hermitian topology here, instead of line gaps [70] or band separation [13], plays an important role in establishing the correspondence.

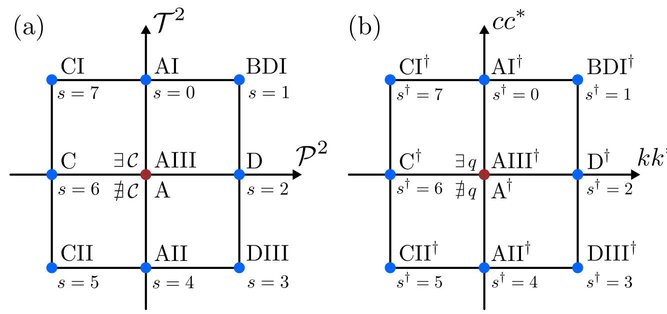

FIG. 2. Diagrams defining (a) Hermitian classes s (b) Non Hermitian real classes $s^\dagger$ (AZ†). Hermitian AZ classes are defined by time reversal $\mathcal{T}$, particle-hole $\mathcal{P}$ and chiral $\mathcal{C}$ symmetries. Similarly, non-Hermitian AZ† classes are defined by K, C and Q-type symmetries. Real (complex) classes are given by blue (red) dots. There are two complex classes ($s = 0, 1$) depending on the absence or presence of $\mathcal{C}$ or q.

$\mathcal{M}$	$\pi_0(\mathcal{M})$	AZ class	NH AZ†	NH AZ
$\mathcal{C}_0$	$\mathbb{Z}$	A (3)	AIII† (3)	AIII (3)
$\mathcal{C}_1$	0	AIII (4)	A† (1)	A (1)
$\mathcal{R}_0$	$\mathbb{Z}$	AI (14)	BDI† (14)	CI (21)
$\mathcal{R}_1$	$\mathbb{Z}_2$	BDI (22)	D† (34)	AI (34)
$\mathcal{R}_2$	$\mathbb{Z}_2$	D (16)	DIII† (19)	BDI (16)
$\mathcal{R}_3$	0	DIII (27)	AII† (7)	D (8)
$\mathcal{R}_4$	$\mathbb{Z}$	AII (15)	CII† (15)	DIII (20)
$\mathcal{R}_5$	0	CII (23)	C† (35)	AII (35)
$\mathcal{R}_6$	0	C (17)	CI† (18)	CII (17)
$\mathcal{R}_7$	0	CI (26)	AI† (6)	C (9)

TABLE I. Classifying spaces $\mathcal{M}$ for Hermitian and non-Hermitian Altland-Zirnbauer (AZ) classes in 0-dimensional systems. The symmetry classes are defined in Fig. 2. For a general d-dimensional system, the classifying space shifts as $\mathcal{R}_s \mapsto \mathcal{R}_{s-d}$. Thus, the classification of d-dimensional Hermitian class s is equivalent to that of $(d+1)$-dimensional NH $s^\dagger$ and NH $(s-2)$ classes. The numbers in the parenthesis show the label used in Ref. [69, 72].

For the above model, the explicit topological invariant $w \in \mathbb{Z}$ is given by

$$w = \int_{-\pi}^{\pi} \frac{dk}{2\pi i}\partial_k \ln(E_k - E_B), \tag{3}$$

which is nothing but the winding number of E_k around the base point E_B [Fig. 1(a,b)]. As a consequence, a nontrivial winding number w implies the existence of modes at $\mathrm{Re}\,E_B$, some with imaginary part above $\mathrm{Im}\,E_B$ and others below $\mathrm{Im}\,E_B$. For the base point choice in Fig. 1(a), $w = 1$ for $t_L > t_R$ and $w = -1$ for $t_L < t_R$. Examining the expressions for the group velocity and imaginary part in the preceding section, we see that w directly corresponds to the number of left-propagating modes minus the number of right-propagating modes, with imaginary part above $\mathrm{Im}\, E_B$, which in turn characterizes the total chirality of long time dynamics. Therefore, the non-Hermitian topological invariant w indeed captures the anomalous dynamics of this model.

Hermitian-Non-Hermitian correspondence— The preceding 1D chiral hopping model hints at a nontrivial connection between non-Hermitian band topology and anomalous dynamics. In particular, the model is reminiscent of the anomalous edge states in a two-dimensional integer quantum Hall state, where the topological invariant $n \in \mathbb{Z}$ characterizes the number of chiral edge modes [Fig. 1(c)]. A similar correspondence has also been pointed out by some of the authors [69] in higher dimensions. Below, we will make this correspondence more rigorous, proving the following general statement:

Proposition For a given d-dimensional anomalous boundary state of a $(d+1)$-dimensional Hermitian system in a symmetry class s, characterized by a topological invariant n, there exists a corresponding d-dimensional non-Hermitian topological system on a closed manifold in the class $s^\dagger$ (and $s-2$) that realizes the same anomalous physics as its long time dynamics, characterized by a non-Hermitian topological invariant n defined with respect to a certain E_B.

Note that since the anomalous boundary theory of the Hermitian system in one higher dimension is defined on a closed manifold, the corresponding non-Hermitian system is also defined on a closed manifold, thus avoiding the non-Hermitian skin effect [5, 36–41]. The exact correspondence is summarized in Tab. I. To understand the table, we need to introduce the following Bernard-LeClair non-Hermitian symmetries [67], which generalize the AZ symmetry classes:

$$H(\mathbf{k}) = \epsilon_q q H^\dagger(\mathbf{k}) q^{-1}, \quad q^2 = \mathbb{I} \quad (Q \text{ sym.}) \quad (4)$$
$$H(-\mathbf{k}) = \epsilon_c c H^T(\mathbf{k}) c^{-1}, \quad cc^* = \eta_c \mathbb{I} \quad (C \text{ sym.}) \quad (5)$$
$$H(-\mathbf{k}) = \epsilon_k k H^*(\mathbf{k}) k^{-1}, \quad kk^* = \eta_k \mathbb{I} \quad (K \text{ sym.}) \quad (6)$$
$$H(\mathbf{k}) = -p H(\mathbf{k}) p^{-1}, \quad p^2 = \mathbb{I} \quad (P \text{ sym.}) \quad (7)$$

where $\epsilon_{\mathcal{O}}, \eta_{\mathcal{O}} \in \{1, -1\}$. These give arise to 38 symmetry classes [69, 70], containing the famous ten-fold AZ classes (two complex classes $s = 0, 1$ and eight real classes $s = 0, 1, ..., 7$, see Fig. 2(a)) as a special case. Instead of dealing with all 38 symmetry classes, we will focus on a subset of them, namely the non-Hermitian (NH) AZ† classes, defined by [70]:

$$k H^*(\mathbf{k}) k^{-1} = -H(-\mathbf{k}) \quad \text{particle-hole } \mathcal{P} \mapsto K, \quad (8)$$
$$c H^T(\mathbf{k}) c^{-1} = H(-\mathbf{k}) \quad \text{time-reversal } \mathcal{T} \mapsto C, \quad (9)$$

where the Hermitian chiral symmetry $\mathcal{C}$, given by the composition of $\mathcal{T}$ and $\mathcal{P}$, is replaced by a Q-type symmetry with $\epsilon_q = -1$, given by the composition of C and K. With these basic symmetries, the complex or real NH classes $s^\dagger$ are defined as in Fig. 2, which show the same "Bott clock" structure as the Hermitian case [66].

To see why this is the natural extension of Hermitian AZ classes, we examine how these non-Hermitian symmetries affect the eigenvalue spectrum. As discussed in Ref. [69, 72], one can prove that the chosen C and K type symmetries affect the structure of eigenvalues as follows:

- Hermitian systems: $\mathcal{P}$ guarantees that eigenvalues appear in a positive and negative pair. $\mathcal{T}$ with $\mathcal{T}^2 = -1$ guarantees the Kramers degeneracy.
- Non-Hermitian systems: K symmetry guarantees that eigenvalues appear in a pair $(\lambda, \epsilon_k \lambda^*)$. In the case of $\epsilon_k = -1$, this corresponds to a pair of complex energies with opposite real part. C symmetry with $cc^* = -1$ guarantees the biorthonormal Kramers degeneracy.

Thus, the spectral consequences of the choice of symmetry in the AZ† classes are consistent with the Hermitian case, justifying the above generalizations to non-Hermitian systems. Interestingly, this symmetry correspondence also naturally arises in the context of non-Hermitian transfer matrices describing the decaying boundary modes of one-dimensional SPTs [72].

We note that one can also define NH AZ classes by switching the roles of complex conjugation and transpose symmetries:

$$c H^T(\mathbf{k}) c^{-1} = -H(-\mathbf{k}) \quad \text{particle-hole } \mathcal{P} \mapsto C, \quad (10)$$
$$k H^*(\mathbf{k}) k^{-1} = H(-\mathbf{k}) \quad \text{time-reversal } \mathcal{T} \mapsto K. \quad (11)$$

Furthermore, a mapping between the classifications of the NH classes $s^\dagger$ and $s-2$ can be explicitly constructed, as summarized in Tab. I. For the proof, see the Supplemental Material [72].

Proof Part I. Dimensional Ascension— We now move on to prove our main proposition. First, we prove the equivalence of the classifications of Hermitian AZ and NH AZ† classes, making use of the fact that the non-Hermitian topology of H with respect to the base point E_B is equivalent to the Hermitian topology of the following doubled Hamiltonian $\bar{H}$ [14] with respect to the zero Fermi energy:

$$\bar{H} = \begin{pmatrix} 0 & H - E_B \\ H^\dagger - E_B^* & 0 \end{pmatrix}. \quad (12)$$

Without loss of generality, we set $E_B = 0$ from now on. $\bar{H}$ should satisfy the corresponding doubled symmetries and an additional chiral symmetry:

$$\bar{c}\bar{H}^*(\mathbf{k})\bar{c}^{-1} = \bar{H}(-\mathbf{k}),$$
$$\bar{k}\bar{H}^*(\mathbf{k})\bar{k}^{-1} = -\bar{H}(-\mathbf{k}),$$
$$\Sigma\bar{H}(\mathbf{k})\Sigma^{-1} = -\bar{H}(\mathbf{k}), \tag{13}$$

where $\bar{k} = I \otimes k$, $\bar{c} = \sigma_x \otimes c$, $\Sigma = \sigma_z \otimes I$, $\bar{k}\bar{k}^* = \eta_k I$, $\bar{c}\bar{c}^* = \eta_c I$.

Let us start with the doubled Hamiltonian $\bar{H}$ of a d-dimensional NH Hamiltonian H in the class $s^\dagger$. Following Teo and Kane [73], we can construct a $(d+1)$-dimensional Hamiltonian by introducing a new momentum-like parameter $-\pi/2 \leq \theta \leq \pi/2$ [74],

$$H_{d+1} = \cos\theta\bar{H} + \sin\theta\Sigma. \tag{14}$$

One immediately sees that this $(d+1)$-dimensional Hermitian Hamiltonian belongs to class s, since

$$\bar{c}H^*_{d+1}(\mathbf{k},\theta)\bar{c}^{-1} = H_{d+1}(-\mathbf{k},-\theta),$$
$$\bar{k}H^*_{d+1}(\mathbf{k},\theta)\bar{k}^{-1} = -H_{d+1}(-\mathbf{k},-\theta), \tag{15}$$

with c corresponding to time-reversal and k corresponding to particle-hole in the AZ† class. Note that Σ is not a symmetry operator anymore. Since $\bar{H}$ and Σ anticommute, the gap for H_{d+1} closes if and only if the gap for $\bar{H}$ closes and $\sin\theta = 0$. Therefore, the classification problems of the Hermitian class s in $(d+1)$ dimensions and the NH class $s^\dagger$ in d dimensions are equivalent. From the mapping between NH AZ and AZ† classes, further equivalence with the NH class $s-2$ follows.

Proof Part II. Dynamical Anomaly— Now that we have established an exact correspondence between Hermitian and non-Hermitian classifications [Tab. I], we turn to investigate the anomalous behavior, and show how a non-Hermitian topological system realizes in its long-time dynamics the anomalous boundary physics of a corresponding Hermitian system. Since anomalous boundary states of Hermitian systems appear as Dirac or Weyl fermions [75], let us consider a boundary state of a topological band structure characterized by a (positive) unit topological invariant, which is given by the following Dirac (or Weyl) Hamiltonian

$$H_{\text{Dirac}}(\mathbf{k}) = k_1\Gamma_1 + \cdots + k_d\Gamma_d, \tag{16}$$

where $\Gamma_{i=1,\ldots,d}$ are Hermitian matrices that satisfy the Clifford algebra $\{\Gamma_i,\Gamma_j\} = 2\delta_{ij}$. Suppose that H_{Dirac} is in the Hermitian AZ class s. Correspondingly, we can construct a NH Hamiltonian in the class $s^\dagger$:

$$H(\mathbf{k}) = i\gamma(\mathbf{k}) + h(\mathbf{k}), \tag{17}$$
$$h(\mathbf{k}) = \sin k_1\Gamma_1 + \cdots + \sin k_d\Gamma_d,$$
$$\gamma(\mathbf{k}) = \cos k_1 + \cdots + \cos k_d - m,$$

with $d-2 < m < d$, so that $\gamma(\mathbf{k})$ is positive at $\mathbf{k} = 0$ and negative at all other time-reversal invariant momenta (TRIM). Here, type K and C symmetries would imply $k\Gamma_i^* + \Gamma_i k = 0$ ($[K,\Gamma_i] = 0$) and $c\Gamma_i^T - \Gamma_i c = 0$ ($\{C,\Gamma_i\} = 0$). This Hamiltonian has a finite complex energy gap over the whole Brillouin zone as long as $\gamma(\mathbf{k}) \neq 0$ at TRIMs. Since H is in class $s^\dagger$, and type K and C symmetries act in the same way as the usual Hermitian symmetries on the Hermitian component $h(\mathbf{k})$ of H, $h(\mathbf{k})$ is in Hermitian class s. Near a TRIM, $h(\mathbf{k})$ describes a Dirac point. Among the 2^d Dirac points at TRIMs, only the Dirac cone at $\mathbf{k} = 0$ survives at long times because only $\gamma(0)$ is positive and all other γ(TRIM)s are negative. Thus, at long times, the non-Hermitian system we have constructed resembles the single Dirac cone anomalous physics of the Hermitian boundary state.

How can this anomalous physics be associated with the nontrivial topology of a non-Hermitian Hamiltonian? To illustrate this, it is sufficient to show that the topology of the corresponding doubled Hamiltonian $\bar{H}$ is nontrivial:

$$\begin{aligned}\bar{H}(\mathbf{k}) &= \tau_x \otimes h(\mathbf{k}) - \tau_y \otimes \gamma(\mathbf{k}) \\ &= \sin k_1\tau_x \otimes \Gamma_1 + \cdots + \sin k_d\tau_x \otimes \Gamma_d \\ &\quad - \tau_y(\cos k_1 + \cdots + \cos k_d - m),\end{aligned} \tag{18}$$

where $\tau_{x,y,z}$ are Pauli matrices. When $d-2 < m < d$, this is the Hamiltonian of the d-dimensional topological insulator in class s with an additional chiral symmetry ($\Sigma = \tau_z$). To see that this Hamiltonian has a unit topological invariant, we consider deformations from the phase with $m > d$, where $\gamma(\mathbf{k})$ is completely negative over the whole Brillouin zone and the system thus lies in the trivial insulator limit. To reach the range $d-2 < m < d$, the band gap goes through the gap closing at $m = d$ at which the system becomes a semimetal with a single Dirac cone at $\mathbf{k} = 0$. Note that this Dirac cone consists of two copies of the symmetry-protected Dirac cone, which can only be gapped as a pair. When the sign of the mass term is reversed at $m = d$, the topological invariant changes by a single unit, so the phase $d-2 < m < d$ has a unit topological invariant. Therefore, a non-Hermitian system carrying nontrivial band topology is topologically equivalent to Eq. (17) that exhibits anomalous dynamics. The correspondence can be easily generalized into an anomalous boundary state with $n > 1$, for example, by using multiple copies of Eq. (17). Moreover, one can also prove conversely that a non-Hermitian system displaying anomalous dynamics of a corresponding Hermitian system must carry nontrivial band topology (see the Supplemental Material [72]). Therefore, there is indeed a rigorous connection between non-Hermitian band topology and its anomalous dynamics. A similar correspondence between the Hermitian class s and the NH class $s-2$ is shown in the Supplemental Material [72].

Example in 2D and General Anomalies— Consider a chiral topological insulator (TI) in 3D belonging to the Hermitian AIII class, characterized by a topological invariant $n \in \mathbb{Z}$ representing the net chirality of boundary

Dirac cones. The corresponding non-Hermitian system is the NH class AIII† in 2D with pseudo-Hermiticity given by $qh^\dagger q^{-1} = -h$. The following NH Hamiltonian belongs to NH class AIII† with $q = \sigma_3$:

$$h(\boldsymbol{k}) = i\gamma_{\boldsymbol{k}} + b_{1,\boldsymbol{k}}\sigma_1 + b_{2,\boldsymbol{k}}\sigma_2 + ib_{3,\boldsymbol{k}}\sigma_3, \tag{19}$$

where $\gamma_{\boldsymbol{k}}, b_{i,\boldsymbol{k}}$ are real functions of $\boldsymbol{k} = (k_x, k_y)$. In Fig. 1(b), the 2D complex dispersion is drawn for a specific choice of parameters. Here, white dots represent Dirac cones, and out of the four Dirac cones, only the one with positive chirality survives at long times in this case, showing that the model corresponds to the boundary of the $n = 1$ 3D chiral TI. However, the Dirac cone is not the most general anomalous feature in the non-Hermitian setting for dimension higher than one. Under non-Hermitian perturbations, it is well known that Dirac cones deform into an exotic exceptional surface structure [26–29] in $d \geq 2$. Indeed, for $b_{3,\boldsymbol{k}} \neq 0$, Dirac cones are deformed to nodal exceptional lines. When both $\gamma_{\boldsymbol{k}}$ and $b_{i,\boldsymbol{k}}$ are odd functions of $\boldsymbol{k}$, the model also belongs to the class AII† with $c = \sigma_2$, which corresponds to the boundary of three-dimensional topological insulators in class AII. In this case, one can show that the number of Dirac cones above E_B is only equivalent modulo two, which agrees with the corresponding Hermitian physics. For detailed discussions with an explicit model, see the Supplemental Material [72].

Conclusion and Outlook— In this Letter, we showed that for a given anomalous boundary of a Hermitian ten-fold class, there is a non-Hermitian bulk system exhibiting the same anomalous dynamics and characterized by a corresponding nontrivial point-gap topology. Our work is in contrast to recent works exploring possible bulk-boundary correspondences in non-Hermitian systems [5, 36–41], as we focus only on the bulk physics of non-Hermitian systems under periodic boundary conditions, a natural choice due to the correspondence with Hermitian anomalous boundary theories. In the Hermitian ten-fold way classifications, topologically protected boundary modes result from multiple bands with non-trivial separations. On the other hand, non-trivial point-gap topology can be well-defined even for a single band, which cannot give rise to a conventional topologically-protected boundary mode. Therefore, instead of point-gap topology, other classes of topology, such as line-gap topology [70], where the topological constraint implies separation between bands, may be a more natural setting to generalize the bulk-boundary correspondence to non-Hermitian systems. Indeed, if this holds, our work may also have interesting extensions to a full correspondence between non-Hermitian point-gap topology and boundary modes of line-gap topology.

J.Y.L. and A.V. are supported by a Simons Investigator Fellowship and by NSF-DMR 1411343. J.A. is supported by IBS-R009-D1. H.Z. is supported by NSF and ARO (W911NF-15-1-0548).

[1] A. Kitaev, in *AIP Conference Proceedings*, Vol. 1134 (AIP, 2009) pp. 22–30, arXiv:0901.2686.
[2] A. P. Schnyder, S. Ryu, A. Furusaki, and A. W. W. Ludwig, Phys. Rev. B **78**, 195125 (2008).
[3] T. Senthil, Annu. Rev. Condens. Matter Phys. **6**, 299 (2015).
[4] C.-K. Chiu, J. C. Teo, A. P. Schnyder, and S. Ryu, Reviews of Modern Physics **88**, 035005 (2016).
[5] V. M. Martinez Alvarez, J. E. Barrios Vargas, M. Berdakin, and L. E. F. Foa Torres, The European Physical Journal Special Topics **227**, 1295 (2018).
[6] N. Hatano and D. R. Nelson, Physical Review Letters **77**, 570 (1996).
[7] M. S. Rudner and L. S. Levitov, Physical Review Letters **102**, 065703 (2009).
[8] K. Esaki, M. Sato, K. Hasebe, and M. Kohmoto, Physical Review B **84**, 205128 (2011).
[9] C. Yuce, Physics Letters A **379**, 1213 (2015).
[10] T. E. Lee, Physical Review Letters **116**, 133903 (2016).
[11] D. Leykam, K. Y. Bliokh, C. Huang, Y. D. Chong, and F. Nori, Physical Review Letters **118**, 040401 (2017).
[12] Y. Xu, S. T. Wang, and L. M. Duan, Physical Review Letters **118**, 045701 (2017).
[13] H. Shen, B. Zhen, and L. Fu, Physical Review Letters **120**, 146402 (2018).
[14] Z. Gong, Y. Ashida, K. Kawabata, K. Takasan, S. Higashikawa, and M. Ueda, Physical Review X **8**, 031079 (2018).
[15] S. Lieu, Physical Review B **97**, 045106 (2018).
[16] S. Lieu, Physical Review B **98**, 115135 (2018).
[17] K. Kawabata, K. Shiozaki, and M. Ueda, Physical Review B **98**, 165148 (2018).
[18] K. Kawabata, S. Higashikawa, Z. Gong, Y. Ashida, and M. Ueda, Nature Communications **10**, 297 (2019).
[19] K. Kawabata, T. Bessho, and M. Sato, arXiv preprint arXiv:1902.08479 (2019).
[20] J. Carlström and E. J. Bergholtz, Physical Review A **98**, 042114 (2018).
[21] K. Takata and M. Notomi, Physical Review Letters **121**, 213902 (2018).
[22] K. Moors, A. A. Zyuzin, A. Y. Zyuzin, R. P. Tiwari, and T. L. Schmidt, Physical Review B **99**, 041116 (2019).
[23] A. A. Zyuzin and A. Y. Zyuzin, Physical Review B **97**, 041203 (2018).
[24] F. K. Kunst and V. Dwivedi, Physical Review B **99**, 245116 (2019).
[25] Z. Yang and J. Hu, Physical Review B **99**, 081102 (2019).
[26] H. Zhou, J. Y. Lee, S. Liu, and B. Zhen, Optica **6**, 190 (2019).
[27] J. C. Budich, J. Carlström, F. K. Kunst, and E. J. Bergholtz, Physical Review B **99**, 041406 (2019).
[28] R. Okugawa and T. Yokoyama, Physical Review B **99**, 041202 (2019).
[29] R. Okugawa and T. Yokoyama, Phys. Rev. B **99**, 041202 (2019).
[30] C. Dembowski, H.-D. Gräf, H. L. Harney, A. Heine, W. D. Heiss, H. Rehfeld, and A. Richter, Physical Review Letters **86**, 787 (2001).
[31] C. Poli, M. Bellec, U. Kuhl, F. Mortessagne, and H. Schomerus, Nature Communications **6**, 6710 (2015).
[32] J. M. Zeuner, M. C. Rechtsman, Y. Plotnik, Y. Lumer,

S. Nolte, M. S. Rudner, M. Segev, and A. Szameit, Physical Review Letters **115**, 040402 (2015).
[33] S. Weimann, M. Kremer, Y. Plotnik, Y. Lumer, S. Nolte, K. G. Makris, M. Segev, M. Rechtsman, and A. Szameit, Nature Materials **16**, 433 (2016).
[34] H. Zhou, C. Peng, Y. Yoon, C. W. Hsu, K. A. Nelson, L. Fu, J. D. Joannopoulos, M. Soljačić, and B. Zhen, Science **359**, 1009 (2018).
[35] A. Cerjan, S. Huang, M. Wang, K. P. Chen, Y. Chong, and M. C. Rechtsman, Nature Photonics (2019), 10.1038/s41566-019-0453-z.
[36] Y. Xiong, Journal of Physics Communications **2**, 035043 (2018).
[37] F. K. Kunst, E. Edvardsson, J. C. Budich, and E. J. Bergholtz, Physical Review Letters **121**, 026808 (2018).
[38] S. Yao and Z. Wang, Physical Review Letters **121**, 086803 (2018).
[39] S. Yao, F. Song, and Z. Wang, Physical Review Letters **121**, 136802 (2018).
[40] C. H. Lee and R. Thomale, Physical Review B **99**, 201103 (2019).
[41] D. S. Borgnia, A. J. Kruchkov, and R.-J. Slager, arXiv preprint arXiv:1902.07217 (2019).
[42] H.-G. Zirnstein, G. Refael, and B. Rosenow, arXiv preprint arXiv:1901.11241 (2019).
[43] L. Herviou, J. H. Bardarson, and N. Regnault, Physical Review A **99**, 052118 (2019).
[44] Z.-Y. Ge, Y.-R. Zhang, T. Liu, S.-W. Li, H. Fan, and F. Nori, arXiv preprint arXiv:1903.09985 (2019).
[45] T. Liu, Y. R. Zhang, Q. Ai, Z. Gong, K. Kawabata, M. Ueda, and F. Nori, Physical Review Letters **122**, 076801 (2019).
[46] S. Longhi, arXiv preprint arXiv:1905.09460 (2019).
[47] Y.-J. Wu and J. Hou, arXiv preprint arXiv:1905.09346 (2019).
[48] C. Yuce, arXiv preprint arXiv:1905.09328 (2019).
[49] K. Yamamoto, M. Nakagawa, K. Adachi, K. Takasan, M. Ueda, and N. Kawakami, arXiv preprint arXiv:1903.04720 (2019).
[50] T.-S. Deng and W. Yi, arXiv preprint arXiv:1903.03811 (2019).
[51] K. Y. Bliokh, D. Leykam, M. Lein, and F. Nori, Nature Communications **10**, 580 (2019).
[52] F. Song, S. Yao, and Z. Wang, arXiv preprint arXiv:1904.08432 (2019).
[53] R. El-Ganainy, K. G. Makris, M. Khajavikhan, Z. H. Musslimani, S. Rotter, and D. N. Christodoulides, Nature Physics **14**, 11 (2018).
[54] V. V. Konotop, J. Yang, and D. A. Zezyulin, Reviews of Modern Physics **88**, 035002 (2016).
[55] H. Cao and J. Wiersig, Reviews of Modern Physics **87**, 61 (2015).
[56] J. Doppler, A. A. Mailybaev, J. Böhm, U. Kuhl, A. Girschik, F. Libisch, T. J. Milburn, P. Rabl, N. Moiseyev, and S. Rotter, Nature **537**, 76 (2016).
[57] H. Xu, D. Mason, L. Jiang, and J. G. E. Harris, Nature **537**, 80 (2016).
[58] S. Lapp, J. Ang'ong'a, F. A. An, and B. Gadway, New Journal of Physics **21**, 045006 (2019).
[59] A. Amir, N. Hatano, and D. R. Nelson, Physical Review E **93**, 042310 (2016).
[60] A. McDonald, T. Pereg-Barnea, and A. Clerk, Physical Review X **8**, 041031 (2018).
[61] F. Lu and Y.-M. Lu, arXiv preprint arXiv:1807.05232 (2018).
[62] H. Kondo, Y. Akagi, and H. Katsura, Phys. Rev. B **99**, 041110 (2019).
[63] V. Kozii and L. Fu, arXiv preprint arXiv:1708.05841 (2017).
[64] T. Yoshida, R. Peters, and N. Kawakami, Physical Review B **98**, 035141 (2018).
[65] A. Altland and M. R. Zirnbauer, Physical Review B **55**, 1142 (1997).
[66] S. Ryu, A. P. Schnyder, A. Furusaki, and A. W. W. Ludwig, New Journal of Physics **12**, 065010 (2010).
[67] D. Bernard and A. LeClair, in *Statistical Field Theories*, edited by A. Cappelli and G. Mussardo (Springer, 2002) arXiv:0110649 [cond-mat].
[68] M. Sato, K. Hasebe, K. Esaki, and M. Kohmoto, Progress of Theoretical Physics **127**, 937 (2012).
[69] H. Zhou and J. Y. Lee, Physical Review B **99**, 235112 (2019).
[70] K. Kawabata, K. Shiozaki, M. Ueda, and M. Sato, arXiv preprint arXiv:1812.09133 (2018).
[71] M. DeMarco and X.-G. Wen, arXiv preprint arXiv:1805.03663 (2018).
[72] See Supplemental Material [url], which includes Refs. [14, 27, 69, 70, 73, 76, 77].
[73] J. C. Teo and C. L. Kane, Physical Review B **82**, 115120 (2010).
[74] θ is a latitude for the higher dimensional Brillouin zone given by the suspension of the original one.
[75] In crystals at $d \geq 4$, this does not hold anymore since the Lorentz symmetry is broken.
[76] R. Jackiw and C. Rebbi, Phys. Rev. D **13**, 3398 (1976).
[77] Y. Ashida and M. Ueda, Phys. Rev. Lett. **120**, 185301 (2018).